Energy Levels of Divalent Thulium in CaF_2

ZOLTAN J. KISS
RCA Laboratories, Princeton, New Jersey
(Received March 15, 1962)

From the fluorescence and absorption spectra of CaF_2:Tm^{2+} an energy-level scheme for the system is proposed. The cubic-crystal-field parameters are determined, and evidence is presented that the $f-f$ transitions are of magnetic-dipole origin. A fluorescent band is observed that appears to originate in closely coupled $Tm^{2+}-Tm^{3+}$ pairs. The large crystal-field splitting in CaF_2:Tm^{2+} is confirmed by the absorption spectra of its isoelectronic systems of CaF_2:Yb^{3+} and CaF_2:Ce^{3+}.

INTRODUCTION

IN the last decade the sharp $f-f$ transitions of the rare earth have been studied successfully in a variety of host materials. In some of these hosts, such as $LaCl_3$,[1] the number of fluorescent and absorption lines can be accounted for by the crystal-field splitting of the spin-orbit multiplets. On the other hand, the spectra in CaF_2 are very much complicated by a large number of satellite lines, which correspond to simultaneous transitions between both the electronic states and the lattice vibrational modes of the crystal. The publications by Feofilov[2] and by Kaiser *et al.*[3] on CaF_2:Sm^{2+} and by Low[4] on CaF_2:Yb^{3+} illustrate well the difficulties of establishing an energy level scheme for the rare-earth ions in CaF_2. Paramagnetic resonance studies[5] have identified the lowest-lying levels of the ground-state multiplet, where this level is paramagnetic, but this technique is insensitive for the determination of large crystal-field splittings. While the announcement of optical-maser operation in CaF_2:Sm^{2+} has given great impetus to the research effort on the CaF_2 system,[6] it did not contribute appreciably to the understanding of its energy level scheme.

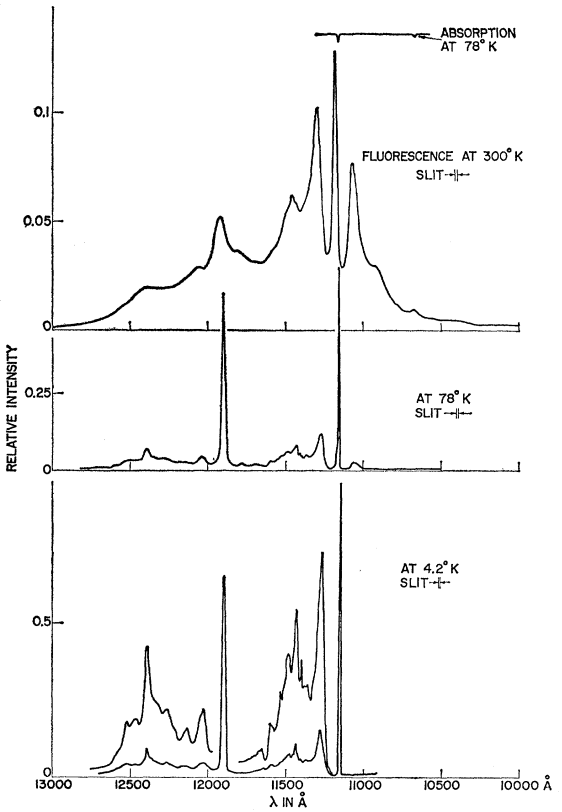

FIG. 1. The fluorescence and absorption spectra of divalent thulium in CaF_2. The initial Tm concentration was 0.05 weight percent thulium fluoride per CaF_2.

In an attempt to determine the crystal-field strength in CaF_2, the simplest rare-earth systems were selected for study, that is, the one-electron system ($4f^1$; Ce^{3+}) and the one-hole system ($4f^{13}$; Yb^{3+} and Tm^{2+}). Since only in the CaF_2:Tm^{2+} system was fluorescence observed, a complete energy-level diagram can only be proposed for this case, but at least it is shown that the absorption data on CaF_2:Yb^{3+} and CaF_2:Ce^{3+} are not inconsistent with the crystal-field splittings suggested by the CaF_2:Tm^{2+} data.

The crystals of CaF_2:Yb^{3+}, CaF_2:Tm^{3+}, and CaF_2:Tm^{2+} were grown at RCA Laboratories, and the CaF_2:Ce^{3+} was purchased from Optovac. CaF_2:Tm^{2+} crystals were also obtained by irradiating with γ rays trivalent thulium in CaF_2, grown by the Stockbarger method. No difference could be found in any of the spectra between the CaF_2:Tm^{2+} crystals obtained by the two different techniques.

ABSORPTION AND FLUORESCENCE SPECTRA

The absorption measurements in the range of 0.2 to 2.5 μ were made on a Cary model 14 spectrometer. The absorption spectra of CaF_2:Ce^{3+} were recorded on a Perkin and Elmer model 12 monochrometer equipped with a LiF prism, and using sapphire windows on the low-temperature Dewar. The fluorescence was studied with a Bausch and Lomb grating monochrometer using the grating in second order with a linear dispersion of

[1] E. Carlson and G. H. Dieke, J. Chem. Phys. **34**, 1609 (1961).

[2] P. P. Feofilov, Optika i Spectroskopiya **1**, 992 (1956).
[3] W. Kaiser, C. G. B. Garrett, and D. L. Wood, Phys. Rev. **123**, 766 (1961).
[4] W. Low, Phys. Rev. **118**, 1608 (1960).
[5] W. Hayes and J. W. Twidell, J. Chem. Phys. **35**, 1521 (1961).
[6] P. P. Sorokin and M. J. Stevenson, IBM J. Research Develop. **5**, 56 (1961).

TABLE I. The frequency and linewidth of the 1.16-μ fluorescent lines at various temperatures.

$T=300°K$			$T=78°K$			$T=4.2°K$			
λ (Å)	(cm^{-1})	$\Delta\nu_{\frac{1}{2}}$ (cm^{-1})	λ (Å)	(cm^{-1})	$\Delta\nu_{\frac{1}{2}}$ (cm^{-1})	λ (Å)	(cm^{-1})	$\Delta\nu_{\frac{1}{2}}$ (cm^{-1})	$\Delta\nu$ (cm^{-1})
10 670	9372								
10 920	9157								
10 700	9116		11 050	9050					
11 185	8941	26	11 153	8966.2	0.86	11 149	8969.5	0.41	
11 300	8849		11 270	8873		11 270	8872		97
						11 370	8789		83
						11 430	8748		41
						11 480	8712		36
						11 600	8621		91
									41
						11 650	8580		
11 930	8383	70	11 890	8410.4	17	11 890	8410.4	12	
12 050	8299		12 030	8313		12 025	8315		95
						12 140	8237		78
						12 260	8157		80
12 400	8065		12 395	8068		12 390	8071		86
									62
						12 470	8019		

33 Å/mm. The signal was synchronously detected with a PbS cell cooled to dry-ice temperature.

The absorption spectra at 78°K and the fluorescence spectra at three temperatures are shown in Fig. 1. The frequency and the linewidth of the various components are given in Table I. The frequencies of the two sharp components are believed to be accurate to $\frac{1}{2}$ cm^{-1} and those of the broader components to 3 cm^{-1}.

The energy-level scheme of the $4f^{13}$ system is relatively simple. The single hole with an orbital angular momentum $l=3$ and spin $s=\frac{1}{2}$ is split into a doublet F state (Fig. 2) by the spin-orbit interaction. By Hund's rule, the lower of the two levels is $^2F_{7/2}$ for the single hole and $^2F_{5/2}$ for the single electron. The cubic field of the CaF_2 splits these states further, the $^2F_{5/2}$ state is split into a double degenerate $E_{5/2}$ and a fourfold degenerate G state, while the $^2F_{7/2}$ state will split into $E_{1/2}$, $E_{5/2}$, and G states. The relative magnitude of the splittings can be calculated in terms of two parameters, λ and μ, as shown in Fig. 2. If the cubic-field potential is expanded in terms of spherical harmonics,

$$V_{\text{cubic}}=V_4+V_6=a\lambda[Y_4^0+(5/14)^{\frac{1}{2}}(Y_4^{-4}+Y_4^4)]+b\mu[Y_6^0-(7/2)^{\frac{1}{2}}(Y_6^{-4}+Y_6^4)],$$

where $a=(4\pi)^{\frac{1}{2}}7\times11/3$, $b=-(4\pi\times13)^{\frac{1}{2}}3\times6\times11/5$, λ is the coefficient proportional to $\langle r^4\rangle$, and μ is proportional to $\langle r^6\rangle$.[7] The point-charge model predicts a positive λ, hence in the upper state the $E_{5/2}$ level is expected to be the lower. The paramagnetic resonance data of Hayes and Twidell[5] established that the lowest level of the ground state has the $E_{5/2}$ symmetry. This only leaves the relative order of the $E_{1/2}$ and G levels of the ground state undetermined.

Electric dipole transitions are forbidden for the f-f transitions since all states of the same configurations have the same parity. On the other hand, magnetic dipole and electric quadrupole operators are of even parity and these transitions are allowed. In this case allowed electric quadrupole transitions are impossible since the selection rule is $\Delta J=0$ and ±2, while the maximum ΔJ possible for the $4f^{13}$ system is $\Delta J=\pm1$. A weak electric dipole transition could still be expected if the selection rule for the free atom is changed by mixing of orbitals with different parity. Van Vleck suggested two possible mechanisms[8] to achieve this: (a) a crystalline field without a center of symmetry, and (b) vibrations that destroy the center of symmetry. The first of these is likely to be absent in the cubic CaF_2 crystal. The two most likely transition mecha-

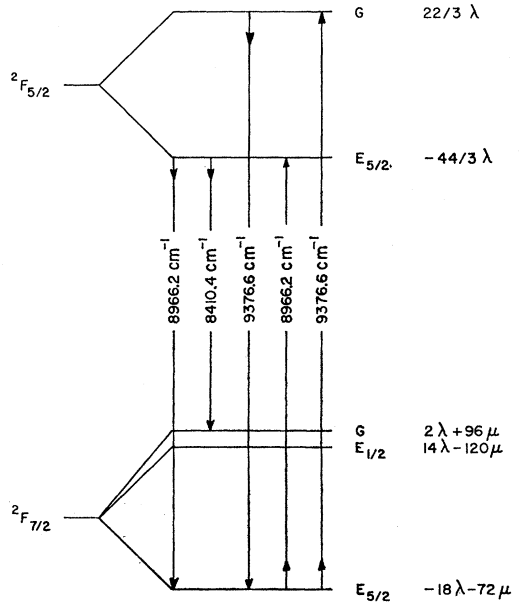

FIG. 2. Energy level diagram of the crystal-field split $4f^{13}$ levels of Tm^{2+} in CaF_2.

[7] The coefficients λ and μ are identical with Pappalardo's $\lambda_{7/2}$ and $\mu_{7/2}$. [See R. Pappalardo, J. Chem. Phys. **34**, 1380 (1961)].

[8] J. H. Van Vleck, J. Phys. Chem. **41**, 67 (1937).

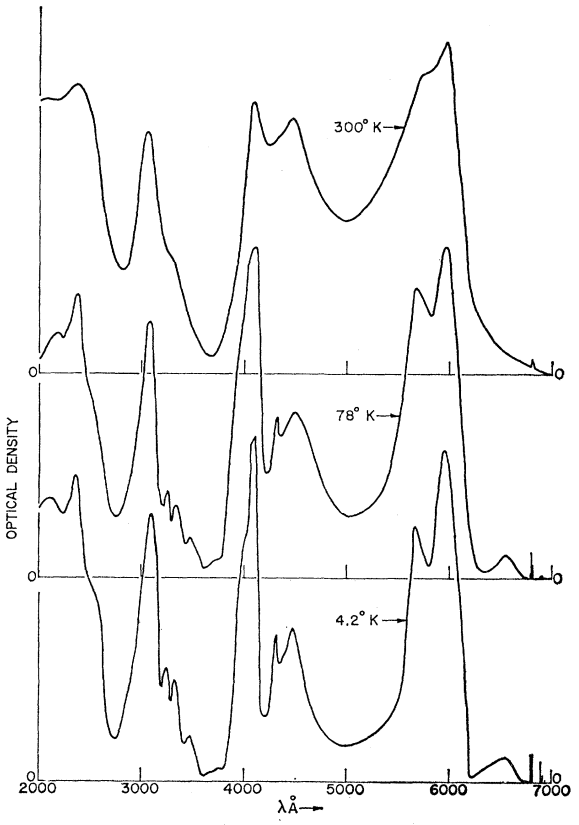

FIG. 3. The broad band absorption of Tm^{2+} in CaF_2 at various temperatures.

nisms therefore are magnetic dipole or vibration induced electric dipole transitions. If the observed fluorescent lines result from electric dipole transitions, from symmetry considerations all six possible transitions are allowed between the two f–f levels, if from magnetic dipole, the $E_{5/2} \rightarrow E_{1/2}$ transition is forbidden.

It is suggested that the two intense lines in Fig. 1 at 8966.2 cm^{-1} and at 8410.4 cm^{-1} are the transitions from the $E_{5/2}$ level of the $^2F_{5/2}$ state to the $E_{5/2}$ and G levels of the ground state, respectively. Transition to the $E_{1/2}$ state does not appear, and the rest of the lines and bands are vibrational satellite lines. The evidence for this interpretation is the following:

(i) In the 78° and 300°K fluorescence spectra Stokes and anti-Stokes vibrational lines with the proper Boltzmann intensity distribution are superimposed on both of these crystal-field lines; e.g., at liquid-N_2 temperature the intensity ratio of the lines separated by about 90 cm^{-1} from the 8966 cm^{-1} line is 0.2, while the predicted ratio is 0.18. Actually the separations of these two lines are not exactly the same, indicating a vibrational energy separation of 84 cm^{-1} in the $^2F_{5/2}$ state and 93 cm^{-1} separation in the $^2F_{7/2}$ state due to slightly different vibrational force constants in the two states.

TABLE II. The fluorescent quantum efficiency. η=number of photons out/number of photons absorbed. Estimated error $=\pm 30\%$.

	8966 cm^{-1} line	8410 cm^{-1} line	Total band
300°K	0.004	0.006	0.04
78°K	0.008	0.015	0.08
4.2°K	0.009	0.015	0.08

(ii) The two strong lines carry the identical satellite structures, although the relative intensities of the various vibrational lines are different. The actual separations at liquid-He temperature are also shown in Table I.

(iii) The sharp vibrational lines are superimposed on a broad band which peaks around 270 cm^{-1} from the strong line. The measured fundamental lattice frequencies[9] of the pure CaF_2 lattice are at 270 cm^{-1} and at 315 cm^{-1}.

The separation of the sharp lines ($\sim$93 cm^{-1}) could possibly correspond to vibrational modes of a thulium–oxygen or thulium–fluorine complex. Replacing the Ca atom by Tm in the CaF_2 system, the reduced mass is increased by more than a factor of 4. Compared to the restrahlen frequency of CaF_2 (270 cm^{-1}), the expected vibrational modes of either of the complexes mentioned would be of the order of 100 cm^{-1}.

Accepting the above identification of the crystal-field lines, the absence of the third line indicates that the lines are of magnetic-dipole origin and the $E_{5/2} \rightarrow E_{1/2}$ transition is forbidden. The separation of the upper $^2F_{5/2}$ state can also be determined from Fig. 1. The lines at 8966.2 and at 9376.6 cm^{-1} show up both in absorption and in fluorescence. If the latter is identified as the $G \rightarrow E_{5/2}$ transition, the splitting of the upper state is 410.4 cm^{-1}. The temperature dependence of the 9376.6-cm^{-1} emission line (assuming that the upper-state populations are in thermal equilibrium) is in good agreement with this separation. From the experimental data the cubic-field parameters can now be determined. They are $\lambda = 18.7$ cm^{-1} and $\mu = 1.08$ cm^{-1}. Using these parameters the position of the $E_{1/2}$ level is predicted to be 9 cm^{-1} below the G level (Fig. 2). One might hope to confirm this energy level scheme by observing the $G \rightarrow G$ and $G \rightarrow E_{1/2}$ transitions in emission at 300°K, but unfortunately these weak transitions come on the steep shoulders of the strong vibrational line at 8873 cm^{-1} and cannot be seen.

The visible strong band-absorption spectra corresponding to the $4f \rightarrow 5d$ or other allowed interconfigurational transitions are shown in Fig. 3. (The sharp line absorptions in the 6800 Å region is the absorption to the $^3F_4$ level of trivalent thulium ions.) The Tm^{2+} fluorescence is excited by pumping in the bands as is shown by the excitation spectra of Fig. 4. This curve was obtained by recording the intensity of a fluorescent line as the spectrum of the pumping source is scanned

[9] G. Heilmann, Z. Naturforsch. **160**, 714 (1961).

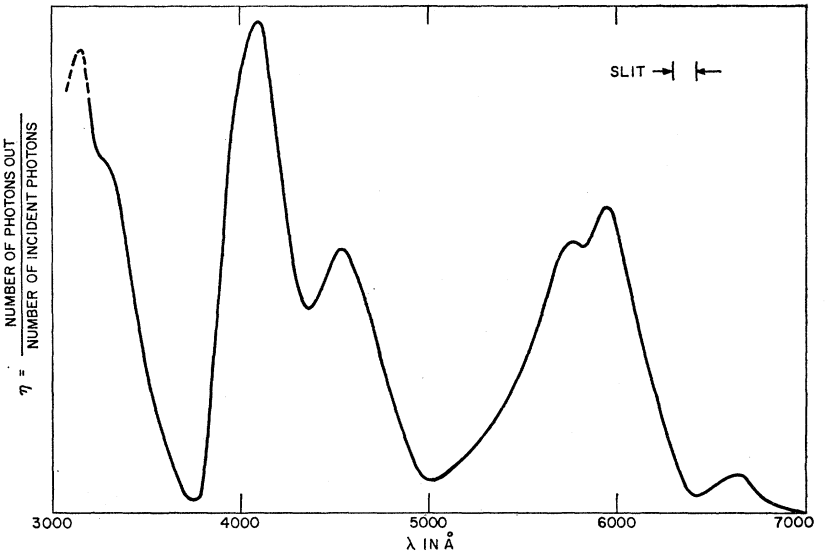

FIG. 4. The excitation spectra of the 1.1- and 1.8-μ fluorescent bands. The ordinate represents the relative number of photons out per incident photon.

with a second monochrometer. The same excitation spectra were found for all the fluorescent lines of Fig. 1. Figure 4 actually shows the relative number of photons out per incident photons, and it can be noted that the shape of this curve is very similar to the absorption curve of Fig. 3. This implies that the fluorescent efficiency η, defined as the number of photons out per number of photons absorbed, does not change much over the bands. This efficiency was measured by pumping in the 6000-Å band and it is given in Table II both for the individual crystal-field lines and for the total band. The energy transfer is inefficient and this may be due partly to the large energy separation between the fluorescing level and the nearest pumping band.

The oscillator strength of a transition can be determined from the absorption intensity using the relation

$$f=\frac{mc^2}{\pi e^2 N}\int \rho(\nu)d\nu,$$

where m and e are the electron mass and charge, N is the number of absorbing ions per cc, and $\int\rho(\nu)d\nu$ is the area under the absorption curve in units of cm^{-2} [i.e., $\rho(\nu)$ is $\log(I_0/I)$ per absorbing length and $d\nu$ is in cm^{-1}]. Allowing for a 40% uncertainty in N, the oscillator strength for the $E_{5/2}\rightarrow E_{5/2}$ transition was found to be $f=1.9\times10^{-8}$ for $N=2.7\times10^{18}$ Tm^{2+} ions per cc. The actual concentration was determined by two methods:

(i) The intensity of the paramagnetic resonance line gave a concentration of $N=8\times10^{18}\pm50\%$ divalent thulium ions per cc.

(ii) If one assumes that a known starting concentration of the doping material will all dissolve in the CaF_2 host as Tm^{3+}, the fraction of thulium that reduces to the divalent state upon irradiation can also be established from the intensity ratios of the trivalent absorption lines before and after irradiation. The concentration by this method was found to be $N=2.7\times10^{18}$ Tm^{2+} ions/cc. The f numbers for some of the other lines and bands are shown in Table III.

The oscillator strength was also determined from the fluorescent lifetime measurements with the formula

$$f=mc^3/8\pi^2e^2\nu^2\tau,$$

where τ is the radiative lifetime. τ can be calculated by dividing the observed fluorescent lifetime by the fluorescent efficiency of the line. The fluorescent lifetime of the $^2F_{5/2}$ state was found to be 2.8×10^{-3} sec at room temperature and 3.6×10^{-3} sec at liquid-N_2 temperature. The calculated f number for the 8966-cm^{-1} line is 3.7×10^{-8}, in good agreement with the value determined from the absorption data.

Thus it seems likely that the f-f transitions in Tm^{2+}:CaF_2 are of magnetic dipole origin as suggested by the observed selection rules and the low value of the oscillator strength of these transitions. Although the fluorescent quantum efficiency of this system is lower and the linewidth broader than that of Sm^{2+}:CaF_2 at liquid-He temperature, the material still appears suitable as a four-level maser oscillator at a frequency of 8410 cm^{-1}.[9a]

TABLE III. The oscillator strength at 78°K.

$\bar{\nu}$ (cm^{-1})	From absorption data	From fluorescent lifetime data
8966.2	1.9×10^{-8}	3.7×10^{-8}
8410.4	0.7×10^{-8}	2.0×10^{-8}
16 600 band	1.7×10^{-3}	

[9a] *Note added in proof.* The CaF_2; Tm^{2+} system was operated as a laser. See Z. J. Kiss and R. C. Duncan, Proc. I.R.E. **50**, 1531 (1962).

THE PUZZLE OF THULIUM

Beside the 1.1-μ fluorescent band of Tm^{2+}, there is also a relatively strong emission band in the region of 1.8 μ as shown in Fig. 5. The excitation spectra for this[9b] band is the same as shown in Fig. 4 indicating that these lines are also pumped in the divalent $4f \rightarrow 5d$ absorption bands. The apparent fluorescent quantum efficiency of this total band is 0.01, an order of magnitude smaller than that of the 1.1-μ band. The frequencies of the various lines are given in Table IV. The two major peaks at liquid N_2 temperature are at 5578 cm^{-1} and at 5170 cm^{-1}, and their separation is 409 cm^{-1} which is the crystal-field splitting of the $^2F_{5/2}$ state. If it is accepted that the fluorescence terminates on the $^2F_{5/2}$ state, this will place the fluorescing level at $5578+8966=14\,544$ cm^{-1} above ground state. This frequency is very close to the observed position of the trivalent absorption line at 6876 Å (Fig. 6). This position is also very near to the beginning of the $f-d$ absorption bands, but it is unlikely that the observed sharp emission could originate in these diffuse bands.

The possibility of emission from an energy level that belongs to a trivalent ion to a level of the divalent ion can only be considered if there is very strong coupling between these two ions, that is if they are nearest neighbors. With completely random distribution of an initial concentration of 0.1 weight percent thulium fluoride in CaF_2, one would expect about 1 Tm per 100 to go in as pair to another nearest-neighbor thulium. If only these pairs are emitting the 1.8-μ band, this would imply a very high quantum efficiency [η_{pair} = (photons out at 1.8 μ/photons absorbed by pair) ≈ 1] for the pair emission.

The energy-level diagrams of divalent and trivalent thulium are shown in Fig. 6. The above evidence suggests that the 1.8-μ band could be the transition from the $^3F_4$ level of Tm^{3+} to the $^2F_{5/2}$ level of Tm^{2+}. Fluorescent lines corresponding to the $^3F_4 \rightarrow {}^2F_{7/2}$ transition in the mixed $Tm^{2+}-Tm^{3+}$ could not be found. The total emission intensity of the 1.1-μ band is proportional to the Tm^{2+} concentration, while that of the 1.8-μ band appears to be proportional to the product of the Tm^{2+} and Tm^{3+} concentration. The relative concentrations of Tm^{2+} and Tm^{3+} were determined from the absorption intensities of the two systems.

The fluorescent lifetime of the emitting state at liquid N_2 temperature was found to be 11.2×10^{-3} sec. Assuming unit quantum efficiency the upper limit of the oscillator strength for the total emission band is $f\sim4\times10^{-6}$, which is the same order of magnitude as the f number of the trivalent transitions as determined

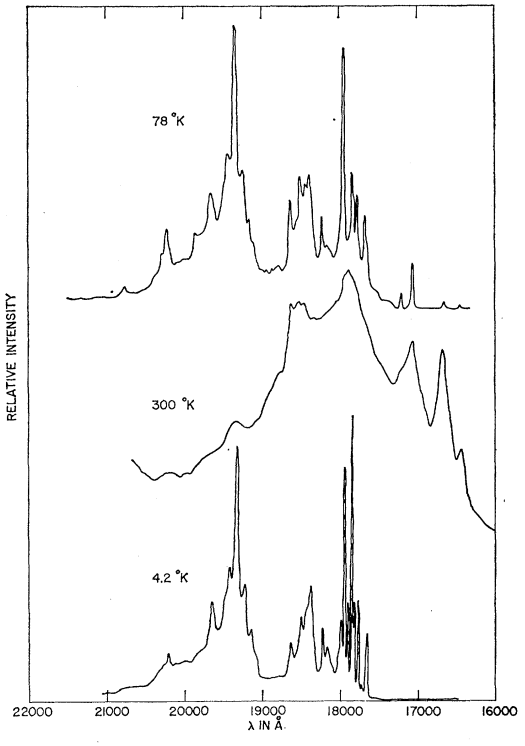

FIG. 5. The 1.8-μ fluorescence of the Tm^{2+}–Tm^{3+} system at three temperatures.

[9b] *Note added in proof.* The above fluorescence of Fig. 5 is different from the pure Tm^{3+} fluorescence, corresponding to the $^3H_5 \rightarrow {}^3H_6$ transition. This trivalent emission was also observed in the range of 1.82–2.0 μ.

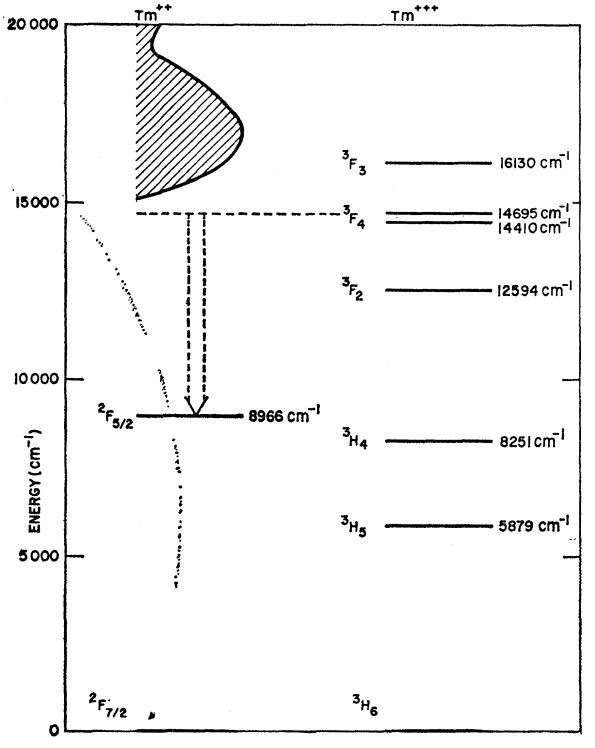

FIG. 6. The energy-level diagram of the Tm^{2+} and Tm^{3+} systems. The dashed arrow represents a transition that could possibly explain the 1.8-μ band fluorescence.

from the intensity of the trivalent absorption lines. These oscillator strengths are available only for absorptions from the ground state and these are, e.g., for the $^3H_6 \rightarrow {}^3F_4$ transition $f=6.1\times10^{-6}$. Work is continuing to elucidate the mechanism of the pair interaction and to explain the observed splitting of the fluorescent terminal state.

THE ABSORPTION SPECTRA OF Yb^{3+} AND Ce^{3+} IN CaF_2

To compare the crystal-field splitting in the other isoelectronic system, the absorption spectra of Yb^{3+} and Ce^{3+} were also studied. The absorption spectra of 0.05 weight percent Yb in CaF_2 are shown in Fig. 7. Large numbers of the Yb ions are in the divalent state as is indicated by a strong divalent band fluorescence in the green identified previously by Butement.[10] The structure of the absorption spectra of Yb^{3+} in CaF_2 varies a great deal depending on the growth conditions. A further paper will follow describing the effects of various possible charge-compensation mechanisms. At present it is only noted that in all the various absorption spectra, the changing structure is superimposed and grouped about two lines; one at 10 240 cm^{-1}, the other at 10 870 cm^{-1}. If these indeed are the two cubic-field split lines of the $^2F_{5/2}$ state, the crystal-field splitting of the upper state is 630 cm^{-1}, slightly larger than that of Tm^{2+}. The cubic-field parameter $\lambda=29$ cm^{-1}, indicating qualitatively the influence of the larger effective nuclear charge. The spin-orbit parameter

TABLE IV. The frequencies and the relative peak intensities of the fluorescent lines in the 1.8-μ region at 300, 78, and 4.2°K. The intensity of the strongest line is taken as 100.

300°K		78°K		4.2°K	
$\bar{\nu}$ (cm^{-1})	I	$\bar{\nu}$ (cm^{-1})	I	$\bar{\nu}$ (cm^{-1})	I
6083	10	6079	2		
5995	70	6002	3		
5858	70	5858	18		
		5814	8		
		5659	30	5666	23
		5627	35	5631	37
				5615	9
5583	100	5602	40	5606	100
				5587	31
		5571	90	5577	80
				5562	8
				5507	6
		5485	30	5489	15
		5438	40	5444	32
5402	80	5402	40	5405	4
		5366	35	5368	5
		5219	6	5225	4
		5198	8	5203	6
5168	30	5168	100	5176	90
		5144	6	5149	6
		5086	15	5092	18
4945	10	4948	25	4951	8
		4820	6		

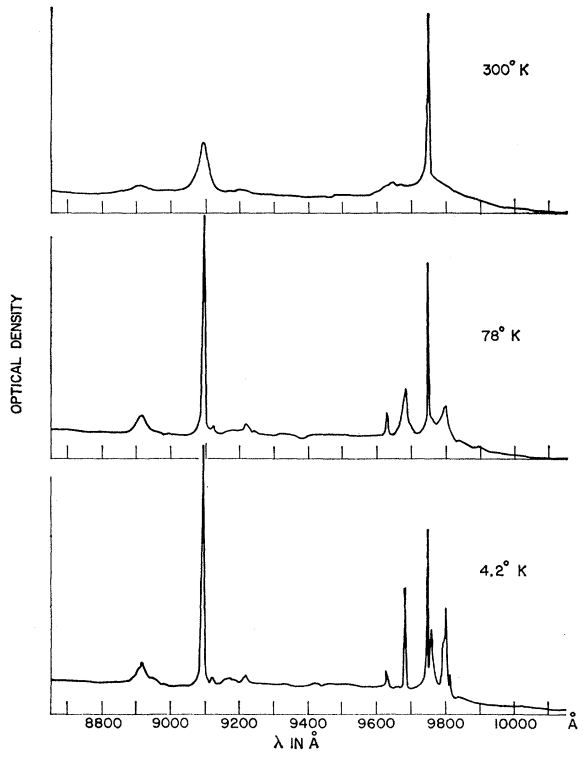

FIG. 7. The absorption spectra of 0.1 weight percent nominal Yb^{3+} concentration in CaF_2 at various temperatures.

[10] F. D. S. Butement, Trans. Faraday Soc. 44, 617 (1948).

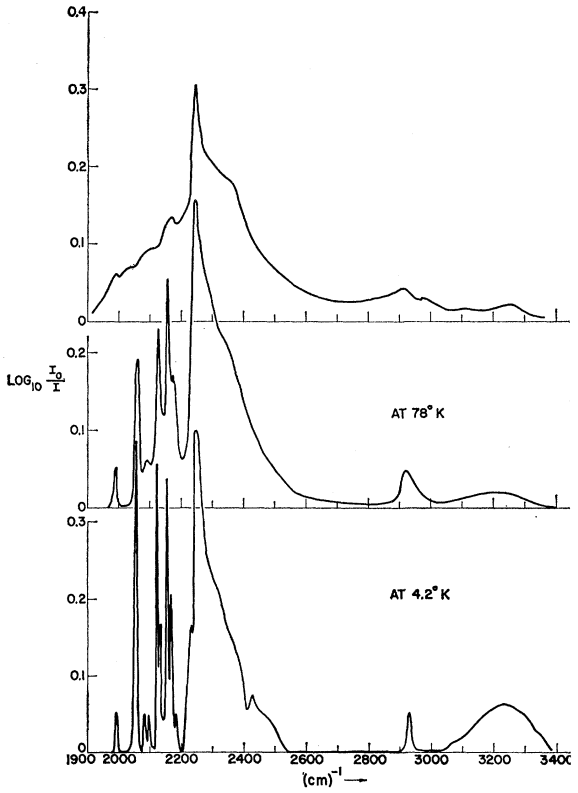

FIG. 8. The absorption spectra of a nominal 0.03 weight percent concentration Ce^{3+} in CaF_2 at 300°, 78° and 4.2°K.

$\zeta_{Yb^{3+}}$ is also larger; the ratio of $\zeta_{Tm^{2+}}/\zeta_{Yb^{3+}}=0.875$. This ratio is very close to the ratio of the other known isoelectronic systems Sm^{2+} and Eu^{3+} where

$$\zeta_{Sm^{2+}}/\zeta_{Eu^{3+}}=0.85.$$

The absorption spectra of 0.03 weight percent trivalent cerium in CaF_2 are shown in Fig. 8. In the case of the $4f^1$ one-electron system, the lowest state is the $^2F_{5/2}$ state and in the cubic field the G level will be the lower, if it is the upper state in the f^{13} system. All the three transitions will be allowed to the three cubic-field split levels of the $^2F_{7/2}$ state whether they are of electric dipole or magnetic dipole origin. Here again, the total extent of the spectra is about 1000 cm^{-1}. At liquid-He temperature there are two broad bands at 2255 cm^{-1} and at 3200 cm^{-1}. These are separated by about 270 cm^{-1} from two sharp lines at 1992 cm^{-1} and at 2930 cm^{-1}, respectively. These sharp lines could possibly be two of the three crystal lines, each carrying the summation tones of the CaF_2 lattice. The position of the third line cannot be determined from the data above. The relative positions of the levels shown in Fig. 2 are certain to change since the crystal field mixing of the two spin-orbit split states becomes very important with the small separation of the two ^2F states. The oscillator strength of the band at liquid-N_2 temperature is $f=7\times10^{-6}$.

While the analysis of the $Yb^{3+}:CaF_2$ and $Ce^{3+}:CaF_2$ system is incomplete, it was presented to show that the proposed large crystal field splitting in $CaF_2:Tm^{2+}$ is not inconsistent with the absorption data of its isoelectronic systems.

ACKNOWLEDGMENTS

It is a pleasure to acknowledge the ready help of D. S. McClure in all phases of the work. Stimulating discussions with S. Polo, C. Struck, and H. Weakliem on the theoretical aspects of the problem were of the greatest value. I also wish to express my gratitude to J. P. Wittke for his continuous cooperation and to H. R. Lewis for the paramagnetic resonance data.

PHYSICAL REVIEW VOLUME 127, NUMBER 3 AUGUST 1, 1962

Nuclear Magnetic Resonance in Cubic Sodium Tungsten Bronzes*

ALBERT NARATH AND DUANE C. WALLACE
Sandia Corporation, Albuquerque, New Mexico

(Received March 12, 1962)

The nuclear magnetic resonances of W^{183} (natural abundance) have been studied in samples of cubic sodium tungsten bronzes (Na_xWO_3) with x ranging from 0.56 to 0.89, in tungsten trioxide, and in tungsten metal. The bronze resonances exhibit appreciable diamagnetic shifts ($\sim$0.3%) with respect to tungsten trioxide, the shift increasing with increasing x. The spin-lattice relaxation time for Na^{23} in $Na_{0.89}WO_3$ was found to be 55 sec. These results provide evidence that the conduction band in the cubic sodium tungsten bronzes is based on tungsten 5d states.

I. INTRODUCTION

THE properties of transition metal oxides have been of much interest in recent years. A large number of these oxides, e.g., TiO, VO_2, etc., are metallic, and much effort has been devoted toward understanding the corresponding electronic transport mechanisms. Of particular interest is tungsten trioxide, WO_3. Although it is an insulator, a number of univalent metals can be added to its lattice to yield metal tungsten bronzes, M_xWO_3 ($0<x<1$) which range from semiconductors to metals, depending on M and x.[1-3] The interest in these materials arises primarily from the fact that the number of conduction electrons can be controlled by adjusting the metal concentration. The most extensively studied bronzes are those for which $M=$Na. In the range of $0.45<x<1$ the sodium tungsten bronzes exhibit typical metallic characteristics such as high electrical conductivity.[1] They crystallize in the cubic perovskite structure in which the tungsten atoms are at the centers of the unit cell, the oxygen atoms at the cube face centers, and the sodium atoms are distributed essentially at random over the corner positions.[4] The WO_3 skeleton of these bronzes is, therefore, almost identical to that of pure WO_3 (which has a distorted cubic structure).[5]

A number of investigations of the electronic properties of Na_xWO_3 have already been reported.[1,3,6-8] In addi-

* This work performed under the auspices of the U. S. Atomic Energy Commission.

[1] L. D. Ellerbeck, H. R. Shanks, P. H. Sidles, and G. C. Danielson, J. Chem. Phys. **35**, 298 (1961).

[2] M. J. Sienko and Thu Ba Nguyen Truong, J. Am. Chem. Soc. **83**, 3939 (1961).

[3] William McNeill and Lawrence E. Conroy, J. Chem. Phys. **36**, 87 (1962).

[4] G. Hagg, Z. Physik. Chem. **B29**, 192 (1935).

[5] G. Hagg and A. Magneli, Revs. Pure and Appl. Chem. **4**, 235 (1954).

[6] W. Gardner and G. C. Danielson, Phys. Rev. **93**, 46 (1954).

[7] R. W. Vest, M. Griffel, and J. F. Smith, J. Chem. Phys. **28**, 293 (1958).

[8] John D. Greiner, Howard R. Shanks, and Duane C. Wallace, J. Chem. Phys. **36**, 772 (1962).